

The spin-orbit angle of the transiting hot jupiter CoRoT-1b[★]

F. Pont¹, M. Endl², W. D. Cochran², S. I. Barnes³, C. Sneden⁴, P. J. MacQueen²
 C. Moutou⁵, S. Aigrain¹, R. Alonso⁶, A. Baglin⁷, F. Bouchy⁸, M. Deleuil⁵,
 M. Fridlund⁹, G. Hébrard¹⁰, A. Hatzes¹¹, T. Mazeh¹², A. Shporer¹²

¹ School of Physics, University of Exeter, Exeter, EX4 4QL, UK

² McDonald Observatory, The University of Texas at Austin, Austin, TX 78731, USA

³ The Anglo-Australian Observatory, 167 Vimiera Rd, Eastwood, NSW 2122, Australia

⁴ Department of Astronomy, The University of Texas at Austin, Austin, TX 78731, USA

⁵ Laboratoire d'Astrophysique de Marseille, UMR 6110, CNRS&Univ. de Provence, 38 rue Frédéric Joliot-Curie, 13388 Marseille Cedex 13, France

⁶ Observatoire de Genève, Université de Genève, 51 Chemin des Maillettes, 1290 Sauverny, Switzerland

⁷ LESIA, CNRS UMR 8109, Observatoire de Paris, 5 place J. Janssen, 92195 Meudon, France

⁸ Observatoire de Haute-Provence, 04870 Saint-Michel l'Observatoire, France

⁹ Research and Scientific Support Department, European Space Agency, ESTEC, 2200 Noordwijk, The Netherlands

¹⁰ Institut d'Astrophysique de Paris, UMR7095 CNRS, Université Pierre & Marie Curie, 98bis boulevard Arago, 75014 Paris, France

¹¹ Thüringer Landessternwarte Tautenburg, Sternwarte 5, 07778 Tautenburg, Germany

¹² School of Physics and Astronomy, Tel Aviv University, Tel Aviv 69978, Israel

ABSTRACT

We measure the angle between the planetary orbit and the stellar rotation axis in the transiting planetary system CoRoT-1, with new HIRES/Keck and FORS/VLT high-accuracy photometry. The data indicate a highly tilted system, with a projected spin-orbit angle $\lambda = 77 \pm 11^\circ$. Systematic uncertainties in the radial velocity data could cause the actual errors to be larger by an unknown amount, and this result needs to be confirmed with further high-accuracy spectroscopic transit measurements. Spin-orbit alignment has now been measured in a dozen extra-solar planetary systems, and several show strong misalignment. The first three misaligned planets were all much more massive than Jupiter and followed eccentric orbits. CoRoT-1, however, is a jovian-mass close-in planet on a circular orbit. If its strong misalignment is confirmed, it would break this pattern. The high occurrence of misaligned systems for several types of planets and orbits favours planet-planet scattering as a mechanism to bring gas giants on very close orbits.

Key words: Planetary systems – Techniques: radial velocities – Techniques: photometric – Stars: individual: CoRoT-Exo-1, CoRoT-1

1 INTRODUCTION

The projection on the plane of the sky of the angle between a planetary orbit and the rotation axis of its host star can be measured in transiting systems, using the Rossiter-McLaughlin (“RM”) effect (Rossiter 1924; McLaughlin 1924). The passage of the planet in front of the star produces an anomaly in the radial velocity curve that depends on this angle. The distribution of spin-orbit angles is an important clue to the formation and evolution mechanisms of planetary systems. Close-in gas giant planets are thought to be formed in a disc and migrate inwards by interaction with the disc (Lin et al. 1996), a scenario expected to produce orbits with generally aligned spin and orbit.

The projected spin-orbit angle has now been measured pre-

cisely for more than a dozen extra-solar planetary systems. Starting with XO-3 (Hébrard et al. 2008), a substantial fraction of these systems exhibit large spin-orbit misalignments (Pont et al. 2009; Johnson et al. 2009). The most extreme case to date is the retrograde orbit of HAT-P-7b (Narita et al. 2009; Winn et al. 2009).

CoRoT-1b¹ (Barge et al. 2008) is the first transiting planet identified by the CoRoT space mission. It is an extreme representative of the “hot Jupiter” family of extra-solar planets, with an orbital period of only 1.5 days. Its mass is similar to that of Jupiter but, like other gas giants on very close orbits, it has a much larger radius ($R \sim 1.4 R_J$). At $V = 13.6$ mag, the parent star lies at the faint end of the magnitude range for presently known planet hosts, so that follow-up observations require large telescopes. As part of

[★] Based on observations obtained at the W.M. Keck Observatory and the European Southern Observatory

¹ Originally known as CoRoT-Exo-1 b. The naming convention for CoRoT planets has been subsequently modified.

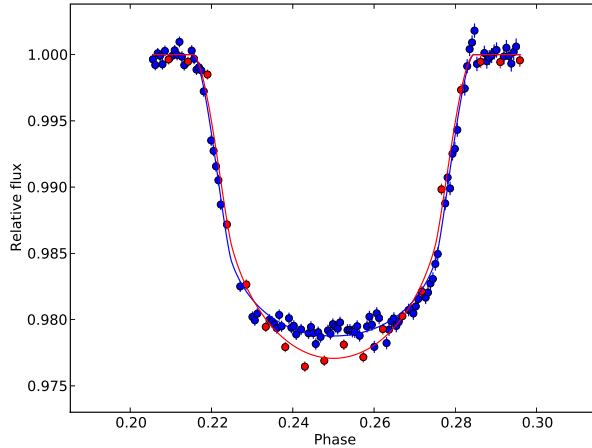


Figure 1. Photometric data from FORS/VLT in the B (squares) and R (circles) filters, with the best-fit transit models.

Date [HJD]	RV [m s ⁻¹]	σ_{RV} [m s ⁻¹]
2454839.930643	-2448.81	17.94
...

Table 1. Radial velocity measurements from HIRES/Keck and HARPS (full table available electronically).

the ground-based follow-up of the CoRoT planet search, new photometric and spectroscopic observations have been gathered on this target, with the objective of refining the system parameters, notably the planet size, of detecting any further longer-period planet in the system, and of measuring the spin-orbit angle through the RM anomaly. We have monitored one transit with the FORS camera on the VLT in two passbands and measured the spectroscopic transit with the HIRES spectrograph on the 10-m Keck telescope. An analysis of the photometric transit curve to constrain the planet size was already presented by Gillon et al. (2009). In this study we concentrate on the determination of the spin-orbit angle from the HIRES data, using the FORS data to constrain the other transit parameters.

2 OBSERVATIONS

2.1 Photometry

The transit was measured in high-accuracy photometry with the FORS camera on the VLT (ESO, Chile) in the *R* and *B* filters on February 27, 2008. The observing strategy and technical details are identical to those described in Pont et al. (2007). The reduction was described in Gillon et al. (2009), and the data is given in Table 2. We chose to alternate between the *R* and *B* filter because the difference in transit lightcurve shape between red and blue wavelengths, caused by the wavelength dependence of the amount of stellar limb darkening, offers a useful complementary constraint on the transit impact parameter, in complement to the shape of the transit ingress and egress. The mean time interval between successive measurements is 78 seconds. The dispersion of the residuals is 0.56 mmag in *R* and 0.52 mmag in *B*, close to the photon-noise limit.

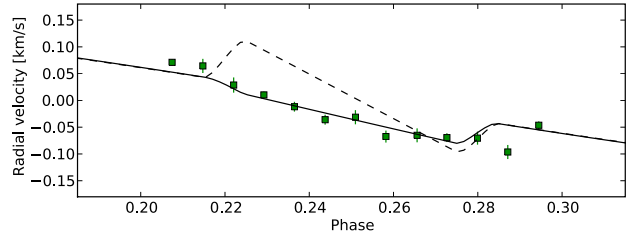


Figure 2. Radial velocity data around the phase of transit. The solid line shows the best-fitting models. The dashed line shows the best fit with $\lambda = 0$ and $V_{\text{rot}} \sin I_s = 5.2 \text{ km s}^{-1}$ imposed.

Date [HJD]	Relative flux	uncertainty	Filter
2454524.556083	0.9996	0.0004	<i>R</i>
...

Table 2. Photometric data from FORS in *B* and *R* (full table available electronically).

2.2 Radial velocity

The radial velocity data comes from the initial follow-up spectroscopy of CoRoT planet candidates with the SOPHIE and HARPS spectrographs, presented in Barge et al. (2008), and a measurement of the spectroscopic transit with the Keck 1 telescope. In addition, we used radial velocity measurements obtained in 2008 with HARPS (ESO Prog. 082C-0.312) to constrain the radial-velocity orbit outside the time of transit.

On 2009 January 8, we used Keck 1 and its HIRES spectrometer to observe the RM effect of CoRoT-1. We used the same instrument setup to measure precise RVs as the California Planet Search group (G. Marcy, priv. comm.). An iodine gas absorption cell is placed in the optical path to provide a precise wavelength calibration. We obtained 13 spectra during the transit with an exposure time of 900 seconds, a slit width of 0.86 arcsec yielding a resolving power of $R \sim 45000$, and a typical S/N ratio of $\approx 40 : 1$ in the iodine region. Precise differential RVs were computed with our *Austral* iodine code (Endl et al. 2000). Table 1 gives the HIRES/Keck and new HARPS radial velocity data.

3 ANALYSIS

The procedure to infer physical parameters from observations of transiting planetary systems has now become standard, and detailed descriptions can be found in the recent literature on the topic (see Winn 2009, for a recent review). A Monte-Carlo Markov Chain (MCMC) algorithm is used to integrate the posterior probability distribution for the model parameters given the observed data and other constraints. Correlated systematics in the data are accounted for by adapting the merit function to include the effect of red noise. Our implementation is described in more details in Pont et al. (2009) and only briefly summarized here. We use the Mandel & Agol (2002) and Ohta et al. (2005) formalisms for the transit and RM effect model curves. The limb-darkening parameters are fixed to the values in Claret (2000). Stellar evolution models (Girardi et al. 2000) are used to constrain the host star's mass and radius. We add a factor in the merit function to take the correlation of the noise into account, using a set of σ_r parameters (Pont et al. 2006), one for each instrument. We use the Metropolis-Hastings jump re-

jection criterion for the MCMC chain, and adopt a chain length of 10^5 . We verified that the correlation length for all fitted parameters is much shorter than the scale length.

Based on the residuals around the model curves, we find that systematics dominate photon-noise uncertainties in the radial velocity data. As discussed in Pont et al. (2006), it is important to take the systematics and their time correlation into account to obtain reliable parameters and uncertainties. The effect of the systematics depends mainly of their correlation in time. There are not enough measurements in the radial-velocity transit sequences to measure the correlation length from the data itself. At the two extremes, we can either assume that the systematics are dominated by timescales very different from the transit duration, or that the systematics are dominated by timescale comparable to the transit duration. If, following Winn et al. (2008), we note β the ratio between the effective uncertainties to be used in the fit to the photon-noise uncertainties, in the first case we have $\beta \simeq \sigma_{\text{res}}/\sigma_{\text{pn}}$, in the second $\beta \simeq n^{1/2}\sigma_{\text{res}}/\sigma_{\text{pn}}$, where σ_{pn} is the photon-noise uncertainty on single data points, σ_{res} the r.m.s. of the residuals, and n the number of measurements during the transit. For our standard solution, we use the first value (negligible time correlation of the radial velocity systematics). In our experience, systematic errors for radial velocity measurements are less strongly correlated in time than photometric errors. We also examine the effect of a higher correlation.

We fit for the following system parameters: four orbital parameters: T_{tr} (epoch of transit), V_0 (centre-of-mass velocity), K (velocity semi-amplitude), i (orbital inclination); mass and radius of the star M_s, R_s ; mass and radius of the planet M_p, R_p ; and projected spin-orbit angle λ . We set the orbital period to the value found from CoRoT photometry, $P = 1.5089557$ days, and the orbital eccentricity to zero. The best constraint on eccentricity comes from the timing of the secondary eclipse, which indicates a negligible eccentricity ($e \cos \omega < 0.01$, Gillon et al. 2009). We use a flat prior in age and metallicity for CoRoT-1, as well as the temperature and stellar rotation velocity measured in Barge et al. (2008): $T_{\text{eff}} = 5950 \pm 50$ K, $V_{\text{rot}} \sin I_s = 5.2 \pm 1.0$ km s $^{-1}$.

4 RESULTS AND DISCUSSION

4.1 System parameters

The best values and central 68% confidence intervals for the parameters of the CoRoT-1 system given by the MCMC integration, in the case assuming uncorrelated radial-velocity systematics, are the following: orbital elements $K = 198 \pm 9$ m s $^{-1}$, $i = 86.7 \pm 0.6^\circ$, $a = 0.0261 \pm 0.0005$ AU, $T_{\text{tr}} = 2454524.6231 \pm 0.0002$ BJD, impact parameter $b = 0.35 \pm 0.08$, star's mass and radius $M_s = 1.03 \pm 0.06 M_\odot$, $R_s = 1.14 \pm 0.03 R_\odot$, planet's mass and radius $M_p = 1.13 \pm 0.07 M_J$, $R_p = 1.48 \pm 0.06 R_J$. We find $\lambda = 77 \pm 11^\circ$ for the projected spin-orbit angle. Figures 1 and 2 compare the data and best-fit model. Figure 2 also shows, for comparison, the best-fit model of the spectroscopic transit with an aligned orbit.

The results on the mass and radius of the star and planet are comparable to previous determinations. Since we use the same values of the spectroscopic parameters of the host star as Barge et al. (2008), a significant update will depend on an improved determination of the spectroscopic parameters.

We discuss below the constraint on the spin-orbit angle of the system.

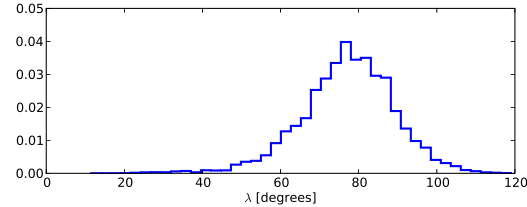


Figure 3. Probability distribution of the projected spin-orbit angle according to the MCMC integration.

4.2 Spin-orbit misalignment

Figures 3 shows the posterior probability distribution function for the projected spin-orbit angle. Our MCMC integration on all available data and constraints favour an angle peaking at $\lambda = +77^\circ$ with a probability distribution well described by a Gaussian with $\sigma \simeq 11^\circ$. In this solution, the star is tilted sideways relative to the planetary orbit, with the planet crossing only the receding side of the star.

Two factors have an important influence on the values derived for the spin-orbit angle: the measured stellar rotation velocity, and the radial velocity measurement systematics during the transit.

Rotation velocity of CoRoT-1

A rotation velocity of $V_{\text{rot}} \sin I_s = 5.2 \pm 1.0$ km s $^{-1}$ is measured from the broadening of the HARPS spectral cross-correlation function (where I_s is the angle between the line-of-sight and the rotation axis of the star, the third angle specifying the spin-orbit configuration, together with λ and planet orbital angle i). Since this constraint has an important influence on the output value for the spin-orbit angle, it is worth examining more closely. A lower value of the rotation would make the relatively flat velocity curve during the transit compatible with lower values for the spin-orbit angle. The measurement of stellar rotation from the broadening of the cross-correlation function has a long pedigree in radial-velocity studies, and the calibration for HARPS is well established. An analysis of the HIRES spectra also indicate significant rotation, $V_{\text{rot}} \sin I_s \simeq 6 \pm 1$ km s $^{-1}$. We therefore consider the determination of the star's projected rotation velocity to be robust.

If the a priori constraint on $V_{\text{rot}} \sin i$ is relaxed, the MCMC integration still converges towards highly tilted spin-orbit angles, with lower values for the rotation velocity in the 2-3 km s $^{-1}$ range. Therefore, the spectroscopic data, especially the Keck velocity curve, favour a high spin-orbit tilt even without external constraint on the stellar rotation velocity.

Red noise in the radial velocity data

As discussed in the case of HD 80606 in Pont et al. (2009), the posterior probability distribution for the spin-orbit angle depends on the choice of the assumptions on the amplitude and timescale of the time-correlated noise in radial velocity during the transit.

If σ_r is of the same order as the expected RM effect (~ 50 m s $^{-1}$), and correlated in time over similar timescales, then obviously the constraint on the spin-orbit angle becomes unreliable.

Since the time series is not much longer than the duration of the transit, it is not possible to determine the correlation timescale on the data itself, but the point-to-point scatter of the HIRES data

System	λ [°]	e
<i>circular and aligned</i>		
HD 189733b	-1.4 ± 1.1	< 0.03
HD 209458b	0.1 ± 2.4	< 0.03
HAT-P-1b	3.7 ± 2.1	< 0.10
CoRoT-Exo-2b	7.2 ± 4.5	< 0.10
HD 149026b	1.9 ± 6.1	< 0.18
TrES-2b	-9.0 ± 12.0	< 0.08
<i>circular and tilted</i>		
CoRoT-1b	77 ± 11	< 0.01
HAT-P-7b	182.5 ± 9.4	~ 0
<i>eccentric and aligned</i>		
HAT-P-2b	1.2 ± 13.4	0.52
HD 17156b	9.4 ± 9.3	0.67
<i>eccentric and tilted</i>		
WASP-14b	-33 ± 7	0.09
XO-3b	37.3 ± 3.7	0.23
HD 80606	39^{+28}_{-13}	0.93

Table 3. Transiting exoplanets with significant projected spin-orbit angle determinations (formal errors smaller than 20°). Angles from the compilation in Fabrycky & Winn (2009), updated with Johnson et al. (2009); Winn et al. (2009) and this paper. Eccentricities from Madhusudhan & Winn (2009), except Joshi et al. (2009) for WASP-14.

seems to indicate correlated systematics on the 10–20 m s^{−1} scale at most. This is similar to the scatter that we found on other targets from the CoRoT follow-up observed with the same instrument.

We have repeated the MCMC integration using a correlation timescale comparable to the duration of the transit. Because the posterior probability distributions are relatively well-behaved and unimodal (see for instance Fig. 3 for the spin-orbit angle), the effect is roughly equivalent to multiplying the parameter uncertainties by a factor $n^{1/2}$. With extreme assumptions on the correlation of the noise ($n = 10$), the result of a spin-orbit misalignment is still significant, but at a reduced level of $\sim 2\sigma$.

Figure 2 compares the radial velocity data with the expected behaviour in case of an aligned orbit, assuming $V_{\text{rot}} \sin I_s = 5.2$ km s^{−1}. Explaining the data with such a model would require not only high systematics, but a remarkable amount of compensation, that we consider unlikely. However, the four data points outside the transit do now follow the model closely, which indicates that we do not have a tight control over the systematics at the point.

One important argument in favour of a strong misalignment is the result from the HARPS spectroscopic transit (Bouchy et al. 2009). Although the HARPS data is more noisy, it also shows a radial velocity constantly *lower* than the Keplerian orbit during the transit, indicating a planet crossing only the receding half of the star.

Precise and high-cadence radial velocity measurements for an object fainter than 13th magnitude in the visible are difficult even with the best instruments and largest telescopes. As for previous cases of measured spin-orbit misalignment, XO-3 (Hébrard et al. 2008; Winn et al. 2009), HD 80606 (Moutou et al. 2009; Winn et al. 2009) and WASP-14 (Johnson et al. 2009), further observations and an independent confirmation of our result will be useful.

4.3 Discussion

The projected spin-orbit angle has now been measured with adequate accuracy for more than a dozen transiting planets. The main result is the strikingly frequent occurrence of high spin-orbit mis-

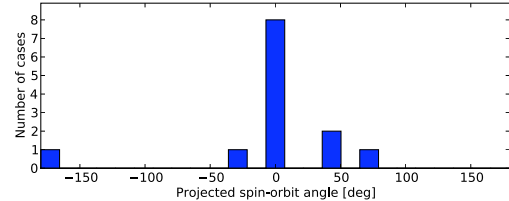


Figure 4. Distribution of projected spin-orbit angles for systems in Table 3.

alignments. At least four systems have spin-orbit tilts in excess of 30 degrees (XO-3, HD 80606, WASP-14, HAT-P-7, see Introduction). Evidence for misalignment may also have been found for WASP-17 (Anderson et al. 2009). According to the data and analysis presented here, CoRoT-1 joins this group, with the radial velocity data favouring an almost polar orbit.

Table 3 displays the systems with significant spin-orbit angle measurements, in relation with orbital eccentricities. Figure 4 shows this list in histogram form. Note that it is important for this ensemble analysis to include only conclusive determinations that do account for correlated noise in the uncertainties. Values with underestimated uncertainties introduce an obvious bias towards non-alignment.

Johnson et al. (2009) pointed out an interesting feature of the first three misaligned systems (XO-3, WASP-14 and HD 80606): all contained a very high-mass gas giants (4, 7 and 12 Jupiter masses) on markedly eccentric orbits. This suggested that misalignment was not a feature of ordinary hot Jupiters, but of their higher-mass cousins. CoRoT-1, however, would break this pattern. It has a mass nearly equal to Jupiter, and a circular orbit. The same is true for HAT-P-7 (Narita et al. 2009; Winn et al. 2009). Therefore the correlation between planet mass, eccentricity and misalignment is called into question.

The cases of CoRoT-1 and HAT-P-7 reinforce the statistical conclusions drawn on an earlier sample by Fabrycky & Winn (2009): the sample as a whole is compatible with a bimodal distribution of spin-orbit angles, with some systems well aligned, and others with little correlation between the two angles. The distribution illustrated by Fig. 4 is compatible with the combination of two sets of system, one with aligned orbits, and the other with randomly oriented orbits. As more systems are measured, most precise statistical properties of the distribution of orbital inclinations for close-in giant planets will become accessible.

An almost polar orbit of CoRoT-1b would be very suggestive of the action of an extreme dynamical event, such as a close encounter with another massive planet. Formation of close-in gas giants by migration in a gas disc would mainly result in aligned orbits (Lin et al. 1996). Gravitational interactions with other bodies can perturb the spin-orbit alignment both during and after the planet formation stage, either through orbital angular momentum exchange (e.g. Kozai mechanism) or more dramatically through catastrophic resonances and close encounters. The first process is, for instance, a plausible explanation for the extremely eccentric system HD 80606. It is less likely to operate on CoRoT-1b, given its close and circular orbit and the absence of detected stellar or planetary perturber. The second type of process is a more likely explanation.

It has long been suggested that planet–planet scattering may account for the presence of close-in exoplanets (Chatterjee et al.

2008; Ford & Rasio 2008). High spin-orbit angles would seem to favour this hypothesis, which has also gained renewed support from other lines of evidence: multiple planetary systems tend to be dynamically dense (Raymond et al. 2009), the distribution of planetary eccentricities resembles that expected from a scattering process (Jurić & Tremaine 2008), and the closest orbital distances conform to the scattering scenario (Ford & Rasio 2006). The case of CoRoT-1 illustrates the high interest of vigorously pursuing the effort to measure the RM anomaly in transiting exoplanets.

ACKNOWLEDGMENTS

We thank Geoff Marcy for providing information on the optimal HIRES setup. We are grateful to the European Southern Observatory for allocation of time to this programme. The Keck observations were made possible by a special allocation of 1 night to the CoRoT Key Science project. The authors wish to recognize the cultural role and reverence that the summit of Mauna Kea has always had within the indigenous Hawaiian community. We are most fortunate to have the opportunity to conduct observations from this mountain.

REFERENCES

Anderson D. R., Hellier C., Gillon M., Triaud A. H. M. J., Smalley B., Hebb L., Collier Cameron A., Maxted P. F. L., Pepe F., Pollacco D., Ségransan D., Udry S., Wilson D. M., 2009, ArXiv e-prints

Barge P., Baglin A., Auvergne M., Rauer H., Léger A., Schneider J., Pont F., Aigrain S., Almenara J.-M., Alonso R., Barbieri M., Bordé P., Bouchy F., Wuchterl G., 2008, *A&A*, 482, L17

Bouchy F., Moutou C., Queloz D., the CoRoT Exoplanet Science Team 2009, ArXiv e-prints

Chatterjee S., Ford E. B., Matsumura S., Rasio F. A., 2008, *ApJ*, 686, 580

Claret A., 2000, *A&A*, 363, 1081

Endl M., Kürster M., Els S., 2000, *A&A*, 362, 585

Fabrycky D. C., Winn J. N., 2009, *ApJ*, 696, 1230

Ford E. B., Rasio F. A., 2006, *ApJ Letters*, 638, L45

Ford E. B., Rasio F. A., 2008, *ApJ*, 686, 621

Gillon M., Demory B. .., Triaud A. H. M. J., Barman T., Hebb L., Montalban J., Maxted P. F. L., Queloz D., Deleuil M., Magain P., 2009, ArXiv e-prints

Girardi L., Bressan A., Bertelli G., Chiosi C., 2000, *A & A SS*, 141, 371

Hébrard G., Bouchy F., Pont F., Loeillet B., Rabus M., Bonfils X., Moutou C., Boisse I., Vidal-Madjar A., 2008, *A&A*, 488, 763

Johnson J. A., Winn J. N., Albrecht S., Howard A. W., Marcy G. W., Gazak J. Z., 2009, ArXiv e-prints

Joshi Y. C., Pollacco D., Cameron A. C., Skillen I., Simpson E., Steele I., Street R. A., Stempels H. C., Christian D. J., Hebb L., Bouchy F., Gibson N. P., 2009, *MNRAS*, 392, 1532

Jurić M., Tremaine S., 2008, *ApJ*, 686, 603

Lin D. N. C., Bodenheimer P., Richardson D. C., 1996, *Nature*, 380, 606

Madhusudhan N., Winn J. N., 2009, *ApJ*, 693, 784

Mandel K., Agol E., 2002, *ApJ Letters*, 580, L171

McLaughlin D. B., 1924, *ApJ*, 60, 22

Moutou C., Hébrard G., Bouchy F., Eggenberger A., Boisse I., Bonfils X., Gravallion D., Ehrenreich D., Forveille T., Delfosse X., Desort M., Vidal-Madjar A., 2009, *A&A*, 498, L5

Narita N., Sato B., Hirano T., Tamura M., 2009, *PASJ*, 61, L35

Ohta Y., Taruya A., Suto Y., 2005, *ApJ*, 622, 1118

Pont F., Hébrard G., Irwin J. M., Bouchy F., Moutou C., Ehrenreich D., Guillot T., Aigrain S., Vidal-Madjar A., 2009, *A&A*, 502, 695

Pont F., Moutou C., Gillon M., Udalski A., Bouchy F., Fernandes J. M., Gieren W., Mayor M., Mazeh T., Minniti D., Melo C., Naef D., Pietrzynski G., Queloz D., Ruiz M. T., Santos N. C., Udry S., 2007, *A&A*, 465, 1069

Pont F., Zucker S., Queloz D., 2006, *MNRAS*, 373, 231

Raymond S. N., Barnes R., Veras D., Armitage P. J., Gorelick N., Greenberg R., 2009, *ApJ Letters*, 696, L98

Rossiter R. A., 1924, *ApJ*, 60, 15

Winn J. N., 2009, in IAU Symposium Vol. 253 of IAU Symposium, Measuring accurate transit parameters. pp 99–109

Winn J. N., Holman M. J., Torres G., McCullough P., Johns-Krull C., Latham D. W., Shporer A., Mazeh T., Garcia-Melendo E., Foote C., Esquerdo G., Everett M., 2008, *ApJ*, 683, 1076

Winn J. N., Howard A. W., Johnson J. A., Marcy G. W., Gazak J. Z., Starkey D., Ford E. B., Colon K. D., Carter J. A., 2009, ArXiv e-prints

Winn J. N., Johnson J. A., Albrecht S., Howard A. W., Marcy G. W., Crossfield I. J., Holman M. J., 2009, ArXiv e-prints

Winn J. N., Johnson J. A., Fabrycky D., Howard A. W., Marcy G. W., Narita N., Crossfield I. J., Suto Y., Turner E. L., Esquerdo G., Holman M. J., 2009, *ApJ*, 700, 302